

Soma Ca^{2+} is decoupled from daily synaptic activity and neuropeptide release in *Drosophila* clock neurons

Highlights

- sLNv clock terminals release the endogenous neuropeptide sNPF at midmorning
- Synaptic sNPF release is evoked by Ca^{2+} influx-dependent spiking at midmorning
- sLNv soma Ca^{2+} peaks at night independently of Ca^{2+} influx without Ca^{2+} spiking
- sLNv soma Ca^{2+} is uncoupled from synaptic release, which evokes delayed behaviors

Authors

Markus K. Klose, Junghun Kim,
Sydney N. Gregg, Brigitte F. Schmidt,
Xiju Xia, Yulong Li, Edwin S. Levitan

Correspondence

levitan@pitt.edu

In brief

Klose et al. demonstrate in sLNv clock terminals that activity-dependent endogenous neuropeptide release occurs at midmorning, many hours after the daily activity-independent Ca^{2+} peak in the soma. Thus, soma Ca^{2+} does not indicate synaptic activity and peptidergic transmission that regulates delayed clock-dependent behaviors.

Report

Soma Ca^{2+} is decoupled from daily synaptic activity and neuropeptide release in *Drosophila* clock neurons

Markus K. Klose,¹ Junghun Kim,¹ Sydney N. Gregg,¹ Brigitte F. Schmidt,² Xiju Xia,^{3,4} Yulong Li,^{3,4} and Edwin S. Levitan^{1,5,*}

¹Department of Pharmacology and Chemical Biology, University of Pittsburgh, Pittsburgh, PA 15261, USA

²Department of Chemistry, Carnegie Mellon University, 4400 Fifth Avenue, Pittsburgh, PA 15213, USA

³State Key Laboratory of Membrane Biology, School of Life Sciences, Peking University, No.5 Yiheyuan Road, Haidian District, Beijing 100871, China

⁴PKU-IDG/McGovern Institute for Brain Research, No.5 Yiheyuan Road, Haidian District, Beijing 100871, China

⁵Lead contact

*Correspondence: levitan@pitt.edu

<https://doi.org/10.1016/j.cub.2025.12.010>

SUMMARY

Drosophila sLNv clock neurons release the co-packaged neuropeptides PDF and sNPF to regulate circadian behaviors and nighttime sleep.^{1–4} Many studies of membrane potential and cytoplasmic Ca^{2+} at the sLNv soma emphasized elevations late at night or in the very early morning,^{5–9} although action potential activity and synaptic release were not quantified. Recently, exocytosis of neuropeptide-containing dense-core vesicles (DCVs) at sLNv terminals was found to peak hours later at midmorning.¹⁰ To resolve the basis of the timing mismatch between somatic measurements and terminal exocytosis, recently developed probes were used to measure daily rhythms in sLNv neuron synaptic Ca^{2+} and sNPF release. Remarkably, at midmorning after soma Ca^{2+} has dropped, both Ca^{2+} spiking and clock-dependent native neuropeptide release peak in the distal terminals of the protocerebrum. Furthermore, Ca^{2+} in the soma and terminals differ in dependence on Ca^{2+} influx. Finally, synaptic DCV exocytosis requires Ca^{2+} spike activity at terminals that is not evident at the soma. These results lead to two striking conclusions. First, soma Ca^{2+} recording, which is the focus of many circuit studies, is not indicative of presynaptic Ca^{2+} and neuropeptide release in distal sLNv terminals. Second, daily clock- and activity-dependent sLNv terminal neuropeptide release occurs many hours in advance of known sLNv neuropeptide effects on nighttime sleep and morning behavior.

RESULTS AND DISCUSSION

sLNv neurons, via their release of PDF, are important morning clock neurons.^{1,4} Thus, for understanding the circadian clock circuit, it is of interest to determine when activity-dependent synaptic neuropeptide release from sLNv terminals occurs during the day. In the absence of direct assays of neuropeptide release, investigators first recorded membrane potential in the sLNv soma. Initial membrane potential recordings from animals raised with an equinox lighting time schedule (LD, 12 h light:12 h dark) showed soma resting membrane potential (RMP) rises at night. However, although action potentials (APs) were observed⁵ and are known to evoke synaptic transmission, their frequency during the day was not reported. More recently,⁹ sLNv RMP and burst incidence were quantified throughout the day, showing that RMP rises during the night and falls during the day, and bursting peaks in an 8-h window (ZT20–4). Representative traces further suggested APs per burst may also change during the day, but AP frequency was not quantified. Similarly, noise analysis of a membrane potential indicator at only two time points (just after lights on vs. just after lights off) showed a widespread increase in the power of the noise spectrum between 1 and 5 Hz at

daybreak.¹¹ However, AP responses of <0.1 s (corresponding to >10 Hz), as well as bursts with durations of seconds,⁹ would not produce power spectrum peaks within the frequency range analyzed, and no perturbations were used to link noise changes to APs. Therefore, because of data acquisition and analysis limitations, membrane potential recordings have not determined when AP activity, the trigger for synaptic transmission, peaks in sLNv neurons.

More recently, soma Ca^{2+} recording has been adopted as a surrogate for activity in many studies. Notably, Liang et al.^{6–8} showed that sLNv soma Ca^{2+} rises at night to produce a broad ~6-h plateau with a peak at ~ZT23. Noise in the soma Ca^{2+} signal of clock neurons was also studied.⁸ For the sLNv recordings, the power spectrum does not show results indicative of APs or their bursts. Furthermore, Ca^{2+} changes were not shown to depend on Ca^{2+} influx, which would be expected if they were produced by AP activity. Therefore, it is not clear that sLNv soma Ca^{2+} , which peaks late at night, reports on the activity that drives synaptic neuropeptide release.

Given this context, it is striking that dense-core vesicle (DCV) exocytosis assayed with an exogenous neuropeptide tagged with a fluorogen-activating protein (Dilp2-FAP)¹² was found to

peak at sLNv terminals at midmorning (ZT3),¹⁰ a time never suggested to be particularly important for sLNv neuron function despite extensive studies of these neurons. However, this timing result might reflect that the exogenous FAP-based indicator does not accurately quantify the exocytosis of native DCVs, which in sLNv terminals contain the neuropeptides PDF and sNPF. Therefore, we set out to measure endogenous neuropeptide release by sLNv terminals based on two recent developments. First, PDF and sNPF were found to be co-packaged together in the same individual DCVs in sLNv neurons.³ This implies that assaying release of either neuropeptide would be sufficient to test if exocytosis timing matched native neuropeptide release. Second, while no sensor for PDF is available, a GPCR-activation-based sensor for detecting sNPF (GRAB_{sNPF1.0}) was developed.¹³ Therefore, GRAB_{sNPF1.0} expression was driven with PDF-GAL4, and sLNv neuron terminals, where neuropeptide-containing DCVs traffic to undergo exocytosis, were imaged for evidence of native neuropeptide release in brain explants.

Native synaptic neuropeptide release by sLNv neurons occurs at midmorning

Validation experiments included demonstrating dose-dependent responses to *Drosophila* sNPF2 (Figure 1A). We then tested for a daily rhythm in GRAB_{sNPF1.0} signals at sLNv terminals. These experiments showed that the peak sNPF signal occurs at ZT3 (Figure 1B), which coincides with DCV exocytosis measured previously.¹⁰ The sNPF peak cannot be attributed to a change in sensor expression because F_{\max} values do not change between ZT23 and ZT3 (Figure 1C). Furthermore, selective knockdown of sNPF expression in sLNv neurons by RNA interference (RNAi) reduced GRAB_{sNPF1.0} fluorescence at ZT3 (Figure 1D). Thus, daily peaks in sNPF sensor fluorescence are the result of neuropeptide release from sLNv neurons rather than other sNPF-expressing neurons in the brain (Figure 1D). Also, application of 100 μM Cd²⁺, which blocks voltage-gated Ca²⁺ channels, inhibited the release peak at ZT3 (Figure 1E). Therefore, Ca²⁺ influx is required for daily synaptic neuropeptide release. Finally, consistent with the control of synaptic neuropeptide content by the circadian clock,¹⁴ the elevated sNPF sensor signal at ZT3 was lost in the *per⁰¹* clock gene amorphic mutant (Figure 1F). Together, the above experiments show that Ca²⁺ influx-evoked endogenous neuropeptide release by sLNv terminals is triggered by the clock at midmorning.

Different Ca²⁺ rhythms in the sLNv soma and terminals

Because the shared midmorning timing of native neuropeptide release (Figure 1) and DCV exocytosis¹⁰ was not predicted from elevations in soma Ca²⁺ and membrane potential,^{5–8} we measured Ca²⁺ in terminals where synaptic neuropeptide release occurs with cytoplasmic GCaMP8f (GC) or synaptotagmin-fused mScarlet3-tagged GCaMP8f (ssGC), which enables ratiometric measurements. With either version of the Ca²⁺ indicator, it was possible to monitor Ca²⁺ changes at ~20 Hz by limiting imaging to the single channel for GCaMP8f (i.e., without changing excitation and emission) at one plane of focus. In the morning, this high-speed imaging of bouton-sized regions of interest (ROIs) in sLNv terminals expressing either GCaMP8f version revealed spontaneous presynaptic Ca²⁺ spikes that display a rapid rise and subsequent slower decay (Figures 2Ai, 2Aii, and

2Bi), which is expected for presynaptic responses to APs.^{15,16} Also consistent with activity responses, inhibiting Ca²⁺ influx with Cd²⁺ application blocked presynaptic Ca²⁺ spike activity within 5 min in every experiment (Figures 2Aii–2Av; $N = 12$). Interestingly, even with a limited field of view, Ca²⁺ signals from regions likely to represent boutons were not always synchronized. For example, in an experiment conducted at ZT3, four patterns of activity were evident among 14 ROIs (Figure S1). This lack of synchrony implies that the four sLNv neurons in each hemibrain are not electrically coupled. Finally, we determined the daily timing of spontaneous Ca²⁺ spike activity with high-speed imaging of ssGC. Strikingly, the frequency of activity varies across the day with a peak of 1.8 ± 0.2 Hz at ZT3 (Figure 2B), at which point all ROIs were active (e.g., Figure S1). Although different behavior from a subset of boutons not viewed in our experiments cannot be excluded without imaging all synaptic sites simultaneously, the detected timing is striking because it corresponds with peak synaptic neuropeptide release (Figure 1B) and DCV exocytosis.¹⁰

The phase disparity between presynaptic Ca²⁺ reported here compared with soma Ca²⁺ reported previously^{6–8} could result from different experimental conditions or be the result of an unexpected disconnect between Ca²⁺ in the soma and terminals. To distinguish between these possibilities, soma Ca²⁺ was measured by ratiometric imaging of ssGC. Measurements in our preparations showed that soma Ca²⁺ peaks at ZT23 and drops during the morning (Figure 3A), in agreement with prior reports.^{6–8} Therefore, experimental conditions do not explain the soma-terminal Ca²⁺ disparity, and peak Ca²⁺ firing frequency in terminals surprisingly occurs while soma Ca²⁺ is dropping.

The disparate Ca²⁺ timing in the soma and terminals reflects different mechanisms operating in the two neuronal compartments. First, while terminal Ca²⁺ spikes and neuropeptide release depend on Ca²⁺ influx (Figures 1 and 2), elevated soma Ca²⁺ at ZT23 measured by ratiometric ssGC imaging persists when Ca²⁺ influx is blocked with Cd²⁺ for 20 min (Figure 3B), indicating that the somatic Ca²⁺ increase does not require Ca²⁺ influx, while terminal Ca²⁺ spikes do. Second, ~20 Hz imaging of the GCaMP channel of GC in a single plane of focus showed sLNv somas did not produce Ca²⁺ spikes at either ZT23 ($N = 8$ somas from 4 hemibrains) when soma Ca²⁺ is elevated or ZT 3 ($N = 18$ somas from 9 hemibrains) when terminal Ca²⁺ spiking is greatest (Figures 2B and 3C). This result was also evident in experiments in which both compartments were studied in a single hemibrain at ZT3 (Figures 3Ci and 3Cii; $N = 4$), thus verifying that the terminal Ca²⁺ spiking is not registered in soma Ca²⁺ recordings. Therefore, different mechanisms, each peaking at different times, govern daily Ca²⁺ elevations in the sLNv neuron soma and terminals. Together, the above data show that synaptic neuropeptide release by sLNv neurons is triggered by spikes of Ca²⁺ influx at midmorning, which contrasts with the spike-free elevation of somatic Ca²⁺ that occurs late at night and does not depend on Ca²⁺ influx.

Peak synaptic activity depletes a large releasable neuropeptide pool

As synaptic neuropeptide release is limited to the peak of activity, we considered why lower frequency activity prior to the peak (e.g., at ZT1) did not elicit neuropeptide release (Figures 1B and

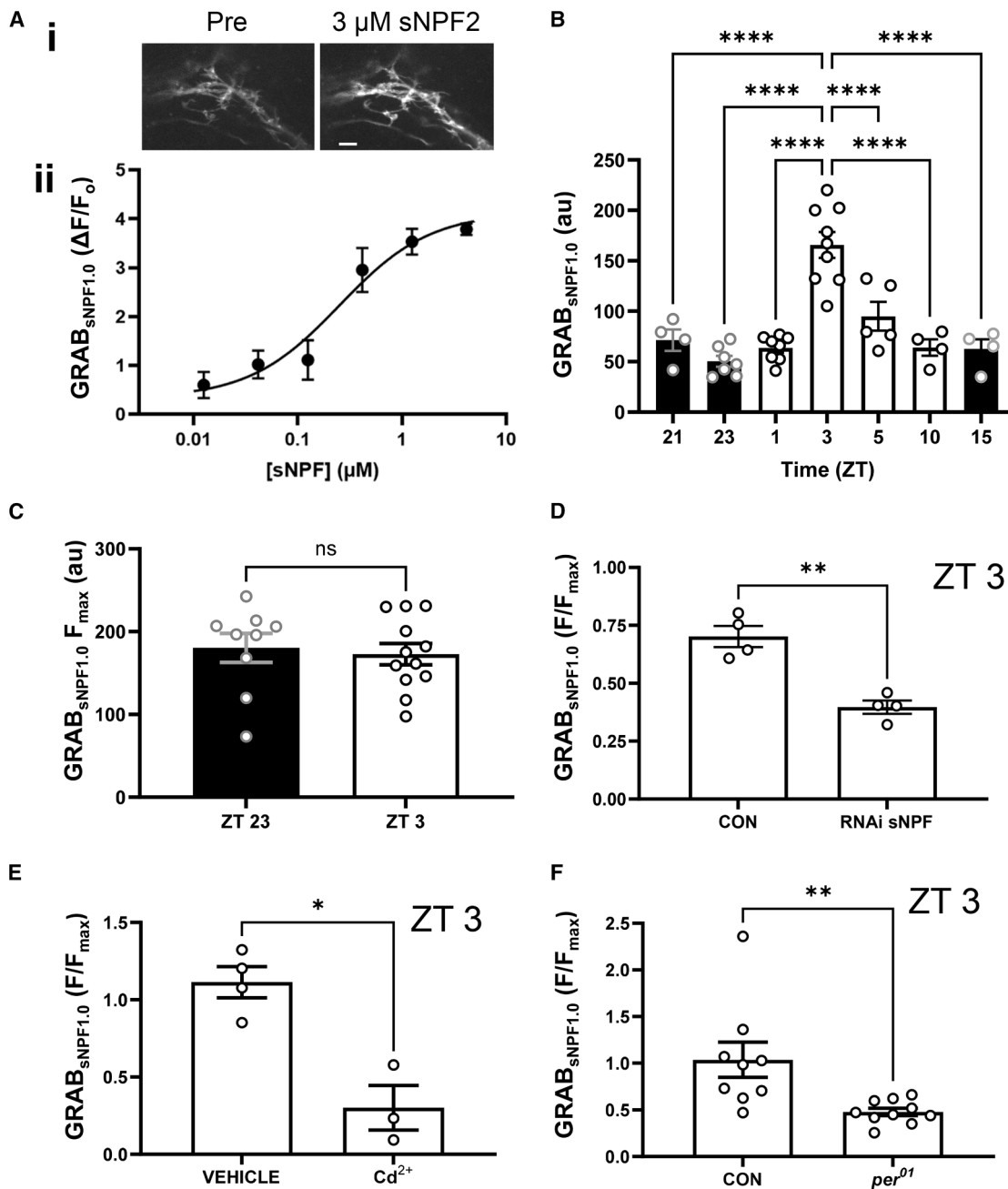


Figure 1. Circadian rhythm of native neuropeptide release from sLNv nerve terminals

(A) (i) $\text{GRAB}_{\text{sNPF}1.0}$ images in sLNv nerve terminals before (pre) and after application of exogenous 3 μM sNPF2 to the brain explant. Shown images are maximum z-projections from image stacks made from 8 $1 \mu\text{m}$ steps. Scale bar, 10 μm . (ii) Dose-response curve for $\text{GRAB}_{\text{sNPF}1.0}$ in LNV neurons in response to various concentrations of sNPF2. Note that responses are expressed as change relative to initial fluorescence (F_0). Error bars here and in subsequent panels show standard error of the mean (SEM).

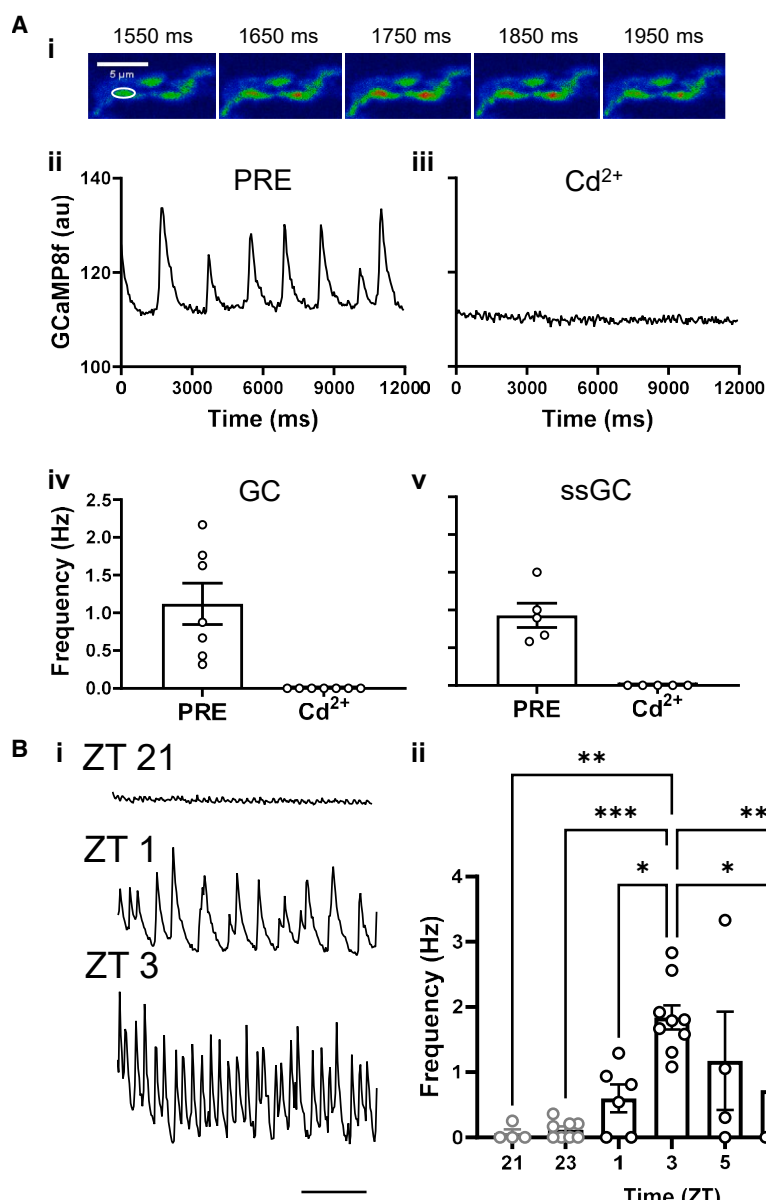
(B) Graph represents average $\text{GRAB}_{\text{sNPF}1.0}$ fluorescence from sLNv nerve terminals at different times of day (ZT) in flies entrained to a 12 h light:12 h dark cycle. One-way ANOVA revealed a significant difference ($p < 0.0001$). Post-test analysis by Dunnett's multiple comparisons test is presented: *** $p < 0.0001$.

(C) The maximal $\text{GRAB}_{\text{sNPF}1.0}$ response evoked by 3 μM (F_{max}) did not change between ZT23 and ZT3. ns, not significant.

(D) $\text{GRAB}_{\text{sNPF}1.0}$ fluorescence at peak release time of day (ZT3) in the sLNv terminals of control UAS- $\text{GRAB}_{\text{sNPF}1.0}$; PDF-GAL4 flies (CON) and UAS-sNPF RNAi/UAS- $\text{GRAB}_{\text{sNPF}1.0}$; PDF-GAL4 flies (RNAi sNPF) (t test, ** $p < 0.01$).

(E) $\text{GRAB}_{\text{sNPF}1.0}$ fluorescence at peak release time of day (ZT3) in the sLNv terminals 60 min after the application of vehicle or ~100 μM cadmium chloride (Cd^{2+}) (t test, * $p < 0.05$).

(F) $\text{GRAB}_{\text{sNPF}1.0}$ fluorescence at peak release time of day (ZT3) in the sLNv terminals in controls and per^{01} flies (t test, ** $p < 0.01$).



2B). First, peak activity might be needed for efficient release because of the superlinear dependence of release on Ca^{2+} . Alternatively, the lower activity prior to the peak may not evoke synaptic release because recently accumulated neuropeptide that occurs in preparation for release^{10,14} by clock-dependent vesicle capture¹⁷ is in DCVs that are not yet competent for release (i.e., because they require priming). To test the latter hypothesis, we bypassed the timing of native activity by inducing depolarization by applying high K^+ saline at ZT1, a time point when synaptic neuropeptide content has already increased, but daily exocytosis has not yet been initiated.¹⁰ For these experiments, DCV exocytosis was measured in animals with cell-specific expression of Dilp2-FAP.¹⁰ Fluorescence of this construct is only produced when extracellular bath-applied membrane-impermeant fluorogen (e.g., MG-Tcarb) passes through the fusion pore formed by kiss-and-run exocytosis

showed that the releasable pool is about half of the total neuropeptide pool in terminals (Figure 4, MGnBu). Thus, at ZT1 there is a large pool of release-competent DCVs in sLNv terminals. Therefore, the clock-dependent timing of release is not due to a change in vesicle release competence but instead reflects the frequency requirement for robust synaptic neuropeptide release and the timing of activity-dependent Ca^{2+} influx that occurs in terminals but not the sLNv soma.

Conclusions

The first conclusion derived from this study is that soma Ca^{2+} recordings, which are often used to infer the timing of neuronal activity, do not always reflect the timing of activity and neurotransmission. For sLNv clock neurons, daily Ca^{2+} elevations in the soma occur without Ca^{2+} influx many hours before presynaptic Ca^{2+} influx-dependent activity and neuropeptide

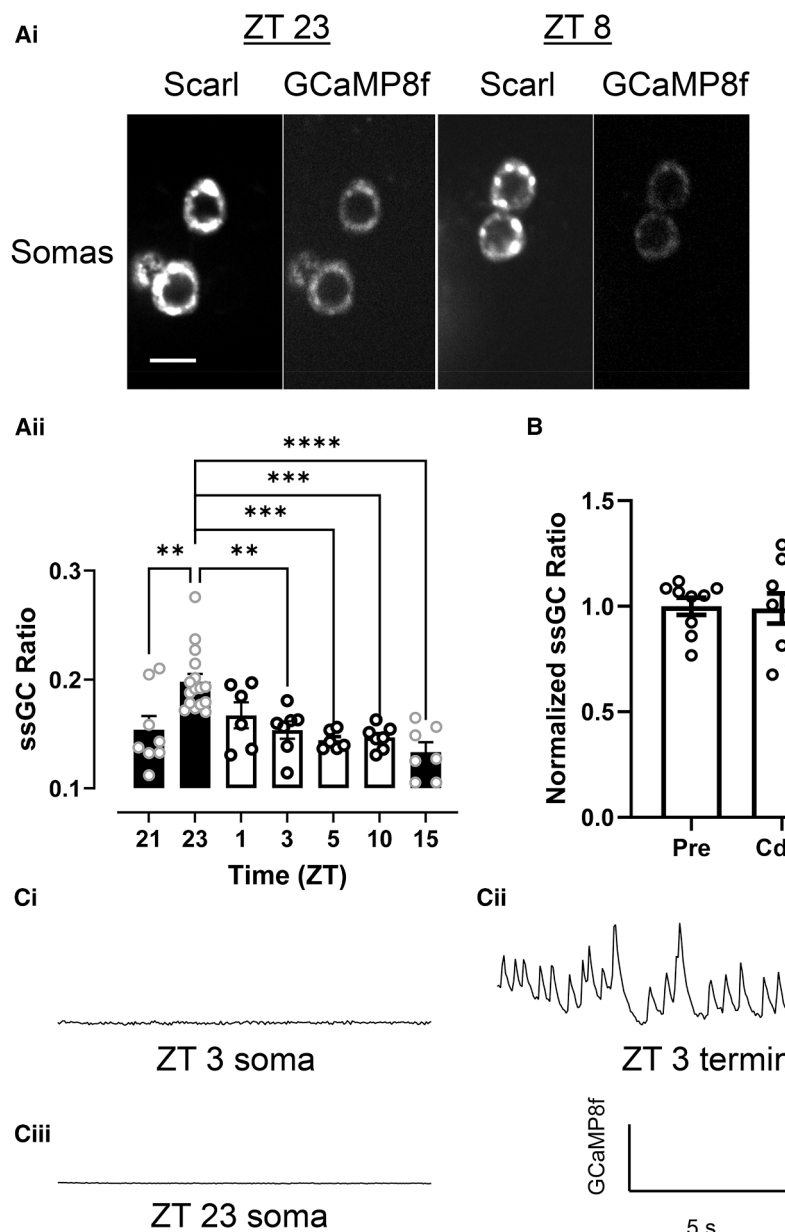
Figure 2. Presynaptic Ca^{2+} imaging in sLNv nerve terminals

(A) (i) Cytoplasmic GCaMP8F driven by PDF-GAL4 in distal sLNv nerve terminals imaged over time at ZT1. Scale bar, 5 μm . (ii) Example trace of GCaMP8F fluorescence data from the ROI shown in (i) measured at ~ 20 Hz in normal HL3 saline prior to adding $\sim 100 \mu\text{M}$ cadmium chloride (Cd^{2+}). (iii) Example trace represents GCaMP8F fluorescence from one ROI after adding Cd^{2+} from the same ROI shown in (i). (iv) Morning (ZT1–5) activity frequency of sLNv nerve terminals expressing GCaMP8F before and after Cd^{2+} ($\sim 100 \mu\text{M}$). Error bars here and in subsequent panels show SEM. (v) Morning (ZT1–5) activity frequency of sLNv nerve terminals expressing Syt-mScarlet3-GCaMP8F (ssGC) before and after Cd^{2+} ($\sim 100 \mu\text{M}$). Note that ZTs were not matched between iv and v.

(B) (i) Syt-mScarlet3-GCaMP8F example traces in distal sLNv nerve terminals imaged over time at ZT21, 1, and 3. The bar indicates 3 s. (ii) Average Ca^{2+} transient frequencies measured in sLNv nerve terminals at different times of day using Syt-mScarlet3-GCaMP8F. One-way ANOVA revealed a significant difference ($p < 0.0001$). Post-test analysis by Dunnett's multiple comparisons test is presented: *** $p < 0.001$, ** $p < 0.01$, * $p < 0.05$. See also Figure S1.

(the predominant mechanism of synaptic neuropeptide release) to bind the fluorogen-activating protein (FAP) inside of the DCV.^{12,18}

Strikingly, DCV exocytosis in response to depolarization is robust at ZT1 (Figure 4, Hi K^+). Furthermore, the exocytosis evoked by depolarization at ZT1 is comparable to peak endogenous exocytosis at ZT3,¹⁰ suggesting endogenous daily release depletes the releasable pool in terminals. To relate release to the total presynaptic pool, a membrane-permeant version of the fluorogen (MGnBu)¹⁹ was applied to label presynaptic Dilp2-FAP in all DCVs. This



release at terminals. We suggest two reasons for the uncoupling of Ca^{2+} between the soma and terminals. First, APs in the sLNv soma occur at a low frequency (≤ 2 Hz) and are small (< 20 mV),^{5,9} reflecting passive backpropagation from the axon initial segment (i.e., where APs initiate), so that they do not efficiently open voltage-gated Ca^{2+} channels. Second, IP₃-IP3R signaling, which releases luminal Ca^{2+} from the endoplasmic reticulum to elevate cytoplasmic Ca^{2+} without relying on extracellular Ca^{2+} influx, is active in sLNv somas at ZT 23.¹⁰ Therefore, the timing of soma Ca^{2+} need not be correlated with activity-dependent peptidergic transmission by sLNv terminals. Uncoupling between the compartments allows Ca^{2+} to be elevated at a different time in the soma to evoke AP-independent effects such as local DCV exocytosis¹⁰ and potentially gene expression. Importantly, these results show circuit activity

Figure 3. Somatic Ca^{2+} regulation in sLNv neurons

(A) (i) ssGC fluorescence images showing the mScarlet and GCaMP8f signals in sLNv somas at ZT23 and ZT8. Scale bar, 5 μm . (ii) GCaMP8f/mScarlet ratios were calculated (ssGC ratio) and graphed at ZT21, 23, 1, 3, 5, 10, and 15 to show soma Ca^{2+} is elevated at night and subsequently decreases throughout the morning. Error bars here and in the subsequent panel show SEM. One-way ANOVA revealed a significant difference ($p < 0.0001$). Post-test analysis by Dunnett's multiple comparisons test is presented: ** $p < 0.01$, *** $p < 0.001$, **** $p < 0.0001$.

(B) Addition of ~ 100 μM CdCl_2 for 20 min at ZT23 had no effect on the soma ssGC ratio, revealing the elevated Ca^{2+} levels at this time were not the result of Ca^{2+} influx.

(C) At ZT 3, when terminals display maximal Ca^{2+} spike frequency, somatic recordings revealed no Ca^{2+} spikes (18 sLNv somas from 9 hemibrains). (i) Cytoplasmic GCaMP8f in sLNv somas reveals no activity, (ii) while sLNv terminals in the same hemibrain revealed Ca^{2+} spike activity (repeated in 4 brains). (iii) At ZT23, no firing was observed in sLNv somas (8 sLNv somas from 4 hemibrains).

cannot be deduced from soma Ca^{2+} imaging with certainty. Thus, circuit models that were formulated based solely on soma Ca^{2+} imaging should be re-evaluated, taking into account the potential for uncoupling between the soma and terminals, which was demonstrated here with a clock neuron.

The second major finding of this study is that clock- and activity-dependent native neuropeptide release from sLNv synapses occurs at midmorning. Therefore, synaptic sNPF release occurs >9 h before nighttime sleep, which is promoted by sNPF from sLNv neurons.² Also, because synaptic PDF is co-packaged with sNPF,³ the rhythmic synaptic release of PDF likely occurs far in advance of PDF-dependent

morning behaviors. The basis for the delay between PDF release and behavior remains to be determined because, while clock circuit connectivity mediated by classical synapses with active zones and small synaptic vesicles has been mapped out, the peptidergic connectome is the subject of speculation based on expression of neuropeptides and receptors without many demonstrated functional interactions.^{20,21} We suggest that a delay between neuropeptide release and behavior might reflect in part the time for induced gene expression effects on evening clock neurons and other targets.^{1,4,22–24} Further downstream communication, also potentially involving neuropeptides, might compound these delays. While delineating the function of the clock circuit without relying on soma Ca^{2+} recordings presents a new challenge, midmorning clock-dependent neuropeptide release by sLNv terminals can now serve as a reference point for clock circuit

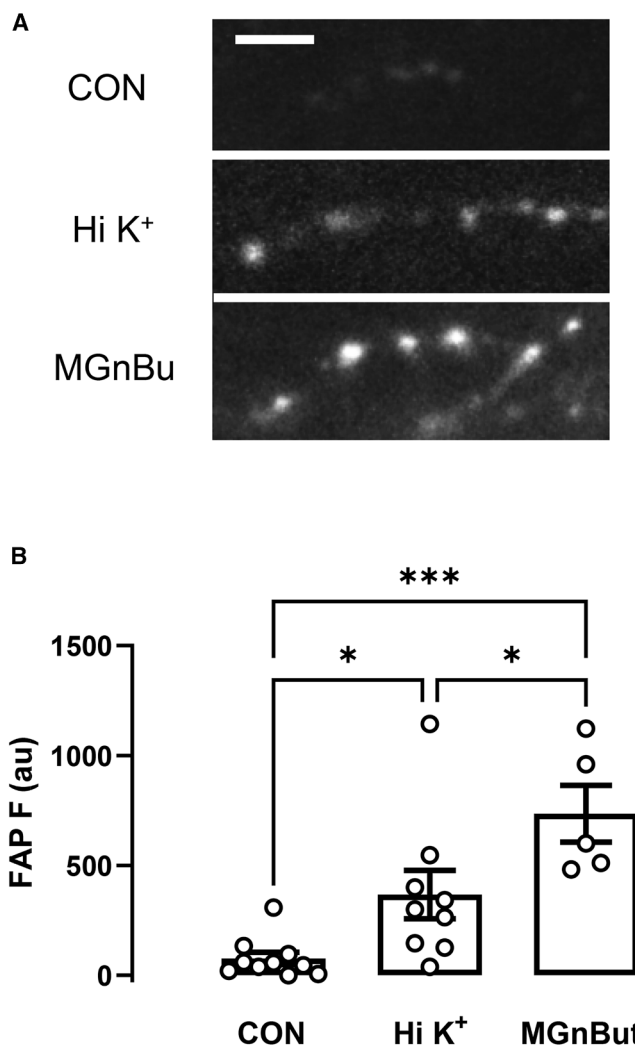


Figure 4. A large releasable pool of DCVs is present at ZT 1 in sLNv nerve terminals

(A) Confocal images of the FAP signal in sLNv nerve terminals exposed to MG-Tcarb in Ca^{2+} -containing HL3 saline (CON), MG-Tcarb in high K^+ saline (Hi K^+), or exposure to the membrane-permeant MG analog MGnBu (500 nM) in Ca^{2+} -containing HL3 saline. Scale bar, 10 μm .

(B) Quantification of FAP-MG fluorescence in sLNv nerve terminals exposed to MG-Tcarb in Ca^{2+} -containing HL3 saline (CON), MG-Tcarb in Hi K^+ saline, or membrane-permeable MGnBu in Ca^{2+} -containing HL3 saline. Error bars show SEM. $n = 10$ for CON; $n = 9$ for Hi K^+ ; $n = 6$ for MGnBu. One-way ANOVA revealed a significant difference ($p < 0.001$). Post-test analysis by Tukey's multiple comparisons test is presented: *** $p < 0.001$, * $p < 0.05$.

function and the aspects of circadian behavior being regulated by events occurring in the dorsal protocerebrum.

RESOURCE AVAILABILITY

Lead contact

Requests for further information and resources should be directed to and will be fulfilled by the lead contact, Edwin Levitan (levitan@pitt.edu).

Materials availability

Drosophila strains used in this manuscript that are not publicly available or easily accessible from stock centers are available upon request to the lead

contact. For fluorogens, contact Brigitte F. Schmidt (bschmidt@andrew.cmu.edu). In some cases, an MTA and/or reasonable payment for maintenance and cost of transport of materials may be required. This study did not generate new, unique reagents.

Data and code availability

- No standardized data types are reported.
- This paper does not report original code.
- All data reported in this paper will be shared by the **lead contact** upon request.

ACKNOWLEDGMENTS

We thank Dion Dickman and Leslie Griffith for flies. Stocks obtained from the Bloomington *Drosophila* Stock Center (supported by NIH grant P40OD018537) were used in this study. We are also thankful for suggestions from Marcel Bruchez (Carnegie Mellon University, deceased) and comments on the manuscript from David Deitcher (Cornell University). Research reported in this publication was supported by the National Institute of Neurological Disorders and Stroke of the National Institutes of Health under award number R01NS032385 to E.S.L. The content is solely the responsibility of the authors and does not necessarily represent the official views of the National Institutes of Health.

AUTHOR CONTRIBUTIONS

M.K.K., J.K., and S.N.G. performed experiments. B.F.S., X.X., and Y.L. provided resources for experiments. M.K.K., J.K., S.N.G., and E.S.L. analyzed data. M.K.K. and E.S.L. formulated experiments, interpreted their results, and wrote the paper.

DECLARATION OF INTERESTS

The authors declare no competing interests.

STAR METHODS

Detailed methods are provided in the online version of this paper and include the following:

- **KEY RESOURCES TABLE**
- **EXPERIMENTAL MODEL AND STUDY PARTICIPANT DETAILS**
- **METHOD DETAILS**
 - Physiology
 - Fly lines
- **QUANTIFICATION AND STATISTICAL ANALYSIS**

SUPPLEMENTAL INFORMATION

Supplemental information can be found online at <https://doi.org/10.1016/j.cub.2025.12.010>.

Received: August 12, 2025

Revised: November 3, 2025

Accepted: December 3, 2025

REFERENCES

1. Crespo-Flores, S.L., and Barber, A.F. (2022). The *Drosophila* circadian clock circuit is a nonhierarchical network of peptidergic oscillators. *Curr. Opin. Insect Sci.* 52, 100944. <https://doi.org/10.1016/j.cois.2022.100944>.
2. Shang, Y., Donelson, N.C., Vecsey, C.G., Guo, F., Rosbash, M., and Griffith, L.C. (2013). Short neuropeptide F is a sleep-promoting inhibitory modulator. *Neuron* 80, 171–183. <https://doi.org/10.1016/j.neuron.2013.07.029>.

3. Yu, J., Zhang, Y., Clements, K., Chen, N., and Griffith, L.C. (2025). Genetically-encoded markers for confocal visualization of single dense core vesicles. *Commun. Biol.* 8, 383. <https://doi.org/10.1038/s42003-025-07829-y>.
4. Sekiguchi, M., Reinhard, N., Fukuda, A., Katoh, S., Rieger, D., Helfrich-Förster, C., and Yoshii, T. (2024). A detailed re-examination of the period gene rescue experiments shows that four to six cryptochrome-positive posterior dorsal clock neurons (DN1p) of *Drosophila melanogaster* can control morning and evening activity. *J. Biol. Rhythms* 39, 463–483. <https://doi.org/10.1177/07487304241263130>.
5. Cao, G., and Nitabach, M.N. (2008). Circadian control of membrane excitability in *Drosophila melanogaster* lateral ventral clock neurons. *J. Neurosci.* 28, 6493–6501. <https://doi.org/10.1523/JNEUROSCI.1503-08.2008>.
6. Liang, X., Holy, T.E., and Taghert, P.H. (2016). Synchronous *Drosophila* circadian pacemakers display nonsynchronous Ca^{2+} rhythms *in vivo*. *Science* 351, 976–981. <https://doi.org/10.1126/science.aad3997>.
7. Liang, X., Holy, T.E., and Taghert, P.H. (2017). A series of suppressive signals within the *Drosophila* circadian neural circuit generates sequential daily outputs. *Neuron* 94, 1173–1189.e4. <https://doi.org/10.1016/j.neuron.2017.05.007>.
8. Liang, X., Holy, T.E., and Taghert, P.H. (2022). Circadian pacemaker neurons display cophasic rhythms in basal calcium level and in fast calcium fluctuations. *Proc. Natl. Acad. Sci. USA* 119, e2109969119. <https://doi.org/10.1073/pnas.2109969119>.
9. Tang, M., Cao, L.H., Yang, T., Ma, S.X., Jing, B.Y., Xiao, N., Xu, S., Leng, K.R., Yang, D., Li, M.T., et al. (2022). An extra-clock ultradian brain oscillator sustains circadian timekeeping. *Sci. Adv.* 8, eab05506. <https://doi.org/10.1126/sciadv.abo5506>.
10. Klose, M.K., Bruchez, M.P., Deitcher, D.L., and Levitan, E.S. (2021). Temporally and spatially partitioned neuropeptide release from individual clock neurons. *Proc. Natl. Acad. Sci. USA* 118, e2101818118. <https://doi.org/10.1073/pnas.2101818118>.
11. Cao, G., Platisa, J., Pieribone, V.A., Raccuglia, D., Kunst, M., and Nitabach, M.N. (2013). Genetically targeted optical electrophysiology in intact neural circuits. *Cell* 154, 904–913. <https://doi.org/10.1016/j.cell.2013.07.027>.
12. Bulgari, D., Deitcher, D.L., Schmidt, B.F., Carpenter, M.A., Szent-Gyorgyi, C., Bruchez, M.P., and Levitan, E.S. (2019). Activity-evoked and spontaneous opening of synaptic fusion pores. *Proc. Natl. Acad. Sci. USA* 116, 17039–17044. <https://doi.org/10.1073/pnas.1905322116>.
13. Xia, X., and Li, Y. (2024). A new GRAB sensor reveals differences in the dynamics and molecular regulation between neuropeptide and neurotransmitter release. Preprint at bioRxiv. <https://doi.org/10.1101/2024.05.22.595424>.
14. Park, J.H., Helfrich-Förster, C., Lee, G., Liu, L., Rosbash, M., and Hall, J.C. (2000). Differential regulation of circadian pacemaker output by separate clock genes in *Drosophila*. *Proc. Natl. Acad. Sci. USA* 97, 3608–3613. <https://doi.org/10.1073/pnas.97.7.3608>.
15. Macleod, G.T., Hegström-Wojtowicz, M., Charlton, M.P., and Atwood, H.L. (2002). Fast calcium signals in *Drosophila* motor neuron terminals. *J. Neurophysiol.* 88, 2659–2663. <https://doi.org/10.1152/jn.00515.2002>.
16. Li, X., Chien, C., Han, Y., Sun, Z., Chen, X., and Dickman, D. (2021). Autocrine inhibition by a glutamate-gated chloride channel mediates pre-synaptic homeostatic depression. *Sci. Adv.* 7, eabj1215. <https://doi.org/10.1126/sciadv.abj1215>.
17. Klose, M.K., Kim, J., Schmidt, B.F., Deitcher, D.L., and Levitan, E.S. (2025). Circadian capture of dense-core vesicles rhythmically boosts pre-synaptic neuropeptide content in a clock neuron. Preprint at bioRxiv. <https://doi.org/10.1101/2025.10.22.684038>.
18. Wong, M.Y., Cavolo, S.L., and Levitan, E.S. (2015). Synaptic neuropeptide release by dynamin-dependent partial release from circulating vesicles. *Mol. Biol. Cell* 26, 2466–2474. <https://doi.org/10.1091/mbc.E15-01-0002>.
19. Perkins, L.A., Fisher, G.W., Naganababu, M., Schmidt, B.F., Mun, F., and Bruchez, M.P. (2018). High-content surface and total expression siRNA kinase library screen with vx-809 treatment reveals kinase targets that enhance F508del-CFTR rescue. *Mol. Pharm.* 15, 759–767. <https://doi.org/10.1021/acs.molpharmaceut.7b00928>.
20. Shafer, O.T., Gutierrez, G.J., Li, K., Mildenhall, A., Spira, D., Marty, J., Lazar, A.A., and Fernandez, M.P. (2022). Connectomic analysis of the *Drosophila* lateral neuron clock cells reveals the synaptic basis of functional pacemaker classes. *eLife* 11, e79139. <https://doi.org/10.7554/eLife.79139>.
21. Reinhard, N., Fukuda, A., Manoli, G., Derksen, E., Saito, A., Möller, G., Sekiguchi, M., Rieger, D., Helfrich-Förster, C., Yoshii, T., et al. (2024). Synaptic connectome of the *Drosophila* circadian clock. *Nat. Commun.* 15, 10392. <https://doi.org/10.1038/s41467-024-54694-0>.
22. Lear, B.C., Zhang, L., and Allada, R. (2009). The neuropeptide PDF acts directly on evening pacemaker neurons to regulate multiple features of circadian behavior. *PLOS Biol.* 7, e1000154. <https://doi.org/10.1371/journal.pbio.1000154>.
23. Lin, Y., Stormo, G.D., and Taghert, P.H. (2004). The neuropeptide pigment-dispersing factor coordinates pacemaker interactions in the *Drosophila* circadian system. *J. Neurosci.* 24, 7951–7957. <https://doi.org/10.1523/JNEUROSCI.2370-04.2004>.
24. Yoshii, T., Wülbeck, C., Sehadova, H., Veleri, S., Bichler, D., Stanewsky, R., and Helfrich-Förster, C. (2009). The neuropeptide pigment-dispersing factor adjusts period and phase of *Drosophila*'s clock. *J. Neurosci.* 29, 2597–2610. <https://doi.org/10.1523/JNEUROSCI.5439-08.2009>.
25. Klose, M., Duvall, L., Li, W., Liang, X., Ren, C., Steinbach, J.H., and Taghert, P.H. (2016). Functional PDF signaling in the *Drosophila* circadian neural circuit is gated by Ral A-dependent modulation. *Neuron* 90, 781–794. <https://doi.org/10.1016/j.neuron.2016.04.002>.
26. Wong, M.Y., Zhou, C., Shakiryanova, D., Lloyd, T.E., Deitcher, D.L., and Levitan, E.S. (2012). Neuropeptide delivery to synapses by long-range vesicle circulation and sporadic capture. *Cell* 148, 1029–1038. <https://doi.org/10.1016/j.cell.2011.12.036>.

STAR★METHODS

KEY RESOURCES TABLE

REAGENT or RESOURCE	SOURCE	IDENTIFIER
Chemicals, peptides, and recombinant proteins		
sNPF2	GenScript Life Science	WFGDVNQKPIRSPSLRFAamide
MG-Tcarb	CMU, Dept. Chem.	bschmidt@andrew.cmu.edu
MGnBu	CMU, Dept. Chem.	bschmidt@andrew.cmu.edu
Experimental models: Organisms/strains		
<i>D. melanogaster</i> : PDF-GAL4	Paul Taghert	N/A
<i>D. melanogaster</i> : UAS-Dilp2-GFP	Edwin Levitan	N/A
<i>D. melanogaster</i> : UAS-Dilp2-FAP	Edwin Levitan	N/A
<i>D. melanogaster</i> : UAS- GRAB _{sNPF1.0}	Yulong Li	BDSC #606553
<i>D. melanogaster</i> : UAS-synaptotagmin::mScarlet3::GCaMP8f	Dion Dickman (JSC)	N/A
<i>D. melanogaster</i> : UAS-GCaMP8f	BDSC:	# 92587
<i>D. melanogaster</i> : w ¹¹¹⁸	Zachary Freyberg	freyberg@pitt.edu
<i>D. melanogaster</i> : UAS-sNPF RNAi (III)	Leslie Griffith	# 15149
<i>D. melanogaster</i> : per ⁰¹	BDSC	# 80917
Software and algorithms		
Image J	Schneider et al. ⁷	https://imagej.net/ij/
Prism 10	Graphpad	RRID: SCR_002798

EXPERIMENTAL MODEL AND STUDY PARTICIPANT DETAILS

Adult *Drosophila* were entrained for at least for 72 hours in a 12-hour light: 12-hour dark (LD) schedule before dissection of 4 to 9 day-old males to generate brain explants. Flies were obtained as described in the key resources table.

METHOD DETAILS

Physiology

Dissections during the dark phase were performed under a red light. Adult flies were immobilized with CO_2 gas and brains were dissected in 0 Ca^{2+} HL3 saline solution (70 mM NaCl, 5 mM KCl, 20 mM $\text{MgCl}_2 \cdot 6\text{H}_2\text{O}$, 115 mM Sucrose, 5 mM Trehalose, 5 mM Hepes, and 10 mM NaHCO_3 , pH 7.3) and then put into polylysine-coated plastic dishes containing HL3 with 2 mM Ca^{2+} for imaging.²⁵ High potassium (Hi K⁺) saline was used to elicit neuropeptide release (2 mM CaCl_2 , 35 mM NaCl, 80 mM KCl, 4 mM $\text{MgCl}_2 \cdot 6\text{H}_2\text{O}$, 65 mM Sucrose, 5 mM Trehalose, 5 mM Hepes, and 10 mM NaHCO_3 , pH 7.3).

All imaging was done on setups with upright Olympus microscopes equipped with a 60× 1.1 NA dipping water immersion objective, a Yokogawa spinning disk confocal head, lasers (i.e., 488 nm laser for GFP illumination, a 561 nm laser for mScarlet3 detection, a 640 nm laser for FAP imaging), and a Teledyne Photometrics sCMOS camera.

Two fluorescent probes were expressed using the PDF-GAL4 driver to image neuropeptide release from sLNv terminals in the dorsal protocerebrum. The first was the sNPF sensor, GRAB_{sNPF1.0},¹³ and the other was Dilp2-FAP,¹² which detects DCV fusion pore opening events. UAS-GRAB_{sNPF1.0} expression in sLNv terminals was used to detect both sNPF endogenous release and application of exogenous sNPF2 (WFGDVNQKPIRSPSLRFAamide) (GenScript Life Science). FAP imaging experiments were performed as previously described.⁶ In the current experiments, a recombinant with UAS-Dilp2-GFP¹⁸ and UAS-Dilp2-FAP was used so that GFP could be used for focusing before application of the fluorogens MG-Tcarb (membrane impermeant) or MGnBu (membrane permeant).¹⁹ Ca^{2+} was imaged with UAS-GCaMP8f (GC) or UAS-syt-mScarlet3-GCaMP8f (ssGC) driven by PDF-GAL4. For resolving Ca^{2+} spikes, green channel data were acquired from a single plane of focus at ~20 Hz. ssGC ratios were recorded at 2 Hz with 100 ms exposures based on alternating between GFP and red optics (i.e., switching between excitation lasers for GCaMP (488 nm) and mScarlet (561 nm) while concurrently changing emission filters with a filter wheel). FAP imaging used Cy5 far red optics (640 nm excitation). Quantification of fluorescence was done in Imagej or Fiji. Statistical analysis (e.g., tests and calculation of standard error of the mean (SEM) for error bars) was performed with Graphpad Prism software.

Fly lines

All flies used the PDF-GAL4 promoter on the third chromosome (provided by Paul Taghert, Washington University in St. Louis). PDF-GAL4 drives expression in the two subsets of clock neuron that express PDF neuropeptide, the small ventrolateral (sLN v) neurons and the large ventrolateral (lLN v) neurons, of which only the sLN v neurons express sNPF. UAS-Dilp2-GFP, UAS-Dilp2-FAP, UAS-GRAB_{sNPF1.0} and UAS-synaptotagmin-mScarlet3-GCaMP8f flies, with the latter coming from Dion Dickman (University of Southern California), were reported previously.^{12,13,16,26} *w¹¹¹⁸* flies were from Zachary Freyberg (University of Pittsburgh), while UAS-sNPF RNAi (III) flies were from Leslie Griffith (Brandies University). Lines from the Bloomington *Drosophila* stock center included *Bl*# 92857 (UAS-GCaMP8f) and *Bl*# 80917 (*per*⁰¹).

QUANTIFICATION AND STATISTICAL ANALYSIS

Statistical analyses were performed using Prism (GraphPad). Bar graphs show means with standard error of the mean indicated by error bars. As indicated in the figure legends, pair-wise comparisons were based on t-tests, while comparisons of multiple experimental groups were based on one-way ANOVA followed by Tukey's or Dunnett's multiple comparisons post-tests. Statistical significance was indicated when two-tail p values were ≤ 0.05 .